ARTICLE

Formaldehyde Free Renewable Thermosetting Foam Based on Biomass Tannin with a Lignin Additive

Bowen Liu[1], Yunxia Zhou[1], Hisham Essawy[2], Shang Feng[1], Xuehui Li[1], Jingjing Liao[1], Xiaojian Zhou[1,3,*], Jun Zhang[1,*] and Sida Xie[1]

[1]Yunnan Provincial Key Laboratory of Wood Adhesives and Glued Products, Southwest Forestry University, Kunming, 650224, China

[2]Department of Polymers and Pigments, National Research Centre, Cairo, 12622, Egypt

[3]Key Laboratory for Forest Resources Conservation and Utilisation in the Southwest Mountains of China (Southwest Forestry University), Ministry of Education, Kunming, 650224, China

*Corresponding Authors: Xiaojian Zhou. Email: xiaojianzhou1982@163.com; Jun Zhang. Email: zj8101274@163.com

ABSTRACT

This study presents easily prepared free formaldehyde bio-based foam based on a prepared thermosetting resin comprising tannin–lignin–furfuryl alcohol-glyoxal (TLFG) via mechanical stirring in presence of ether as a foaming agent. The foam was developed through a co-polycondensation reaction of glyoxal and furfuryl alcohol with condensed tannin and lignin, which is a forest-derived product. Investigation using scanning electron microscopy (SEM) showed more closed-cell structure without cracks and collapse in the TLFG foam, with a higher apparent density with respect to tannin–furanic–formaldehyde (TFF) foam. Differential scanning calorimetry (DSC), dynamic thermomechanical analysis (DTMA), and thermogravimetric analysis (TGA) investigations revealed that the curing process of TLFG foam proceeds easily even at a lower temperature. Additionally, it acquired higher heat resistance than TFF foam. Moreover, TLFG has a more robust chemical network structure, which contributes efficiently to the mechanical strength and a lower pulverization degree compared with TFF-derived foam. Fourier transform infrared spectrometry (FTIR) and electrospray ionization mass spectrometry (ESI-MS) proved that the cross-inking reactions between tannin, lignin, furfuryl alcohol, and glyoxal have been proceeded efficiently.

KEYWORDS

Foam materials; heat resistance; tannin; lignin; glyoxal; compressive strength

1 Introduction

Foams, such as polyurethane, polystyrene, phenolic, and polyethylene, have been widely used in building, packaging, automobile, and other fields due to their excellent thermal insulation, sound resistance and cushioning properties [1–4]. However, these foams are synthesized with non-renewable raw materials and contain toxic substances, which limit their future development. Condensed tannin, mainly extracted from wood bark [5], is the most abundant natural aromatic biomolecules source after lignin. The cross-linking between tannin and furfuryl alcohol, which is the major chemical commodity produced from furfural obtained from the hydrolysis of residues of corn and wheat, has been established

under acidic conditions in the pH rang of 2–5 to obtain tannin–furanic (TF) foam with attractive properties, such as lightweight, excellent fire resistance, thermal insulation, and thermal-cold cycling expansion behavior [6–10]. However, the reaction of self-condensation of furfuryl alcohol had been established under acidic conditions, which predominates to such an extent that leads to little or no co-reaction with tannin [11,12]. Besides, when the mass ratio of furfuryl alcohol to condensed tannin is very high, a high cost becomes a problem. Moreover, furfuryl alcohol has no obvious reaction activity under alkaline conditions in the pH rang of 8–11, whereas the self-polycondensation reaction and hydroxymethylation mainly occur under acidic conditions [13]. To improve the reactivity of tannin and furfuryl alcohol, formaldehyde was used to cross-link tannin and facilitates the obtainment of tannin–furanic–formaldehyde (TFF) foam with good mechanical properties [14]. However, the toxicity associated with free formaldehyde and health hazard problems limit its further development. A previous study showed a possible complete substitution of formaldehyde with glyoxal or glutaraldehyde, it could be used as a cross-linker to react with furfuryl alcohol and tannin under acidic conditions [15]. However, the hardness and compressive strength became lower with glyoxal or glutaraldehyde compared with formaldehyde because the polymerization among cells did not occur quickly enough, thereby leading to gas bubbles coalescence during foam blowing process and a high pulverization degree was observed. Additionally, lignin, the main byproduct of pulp and paper industries, is an abundant, cheap, renewable, and nontoxic natural polymer with a cheaper price than that of tannin [16–20]. The main structure of lignin comprises p-hydroxyphenyl propane, guaiacyl, and syringyl (shown in Figs. 1a–1c, respectively). It can be used as a reinforcing agent to improve the mechanical properties of the tannin–furanic based foam because its structure is similar to that of tannin [21]. However, it was reported that the low reactivity and complex structure of lignin caused few or no cross-linking activity with tannin and furfuryl alcohol, forcing the curing temperature of foam preparation to be as high as 373 K [21]. In the previous study [12,22], it was found that the use of glyoxal as a cross-linking agent can establish a link with para-carbon of hydroxymethyl of furfural alcohol, and it can further react with lignin and tannin to improve the cross-linking of the overall resin system. Consequently, studies on tannin, lignin, furfuryl alcohol, and glyoxal have been conducted to realize the feasibility of tannin–furfuryl alcohol-glyoxal-lignin (TFLG) resin-based foam with high pulverization degree and good mechanical properties. Currently, tannin–furan foam is prepared via a low boiling point liquid foaming method using ether as a foaming agent [23]. Foams can be quickly prepared without heating. However, the foaming process is difficult to control under such a case leading to a foam with irregular distribution of pores, which is not good for application. We suggested in a previous study [24] that the addition of Tween 80 as an emulsifier into tannin–furanic resin system can change the interfacial tension of the molten polymer to produce wrapping of the gas bubbles, which is essential for preparation of foams with a uniform distribution of pores. Therefore, in this study, furfuryl alcohol and glyoxal were employed to cross-link under acidic conditions. Then, tannin and lignin were added to the resin system to co-condense with the resin leading to a complicated matrix. Finally, ether (as blowing agent) and Tween 80 (as an emulsifier) were mixed with the resin matrix under mechanical stirring thus air was wrapped and a foam with a uniform distribution of pores was obtained after heating, curing, and drying. This study presents an essential methodology for development of an environmental-friendly foam with high pulverization degree, which is potentially to replace the industrially applicable oil-derived foam.
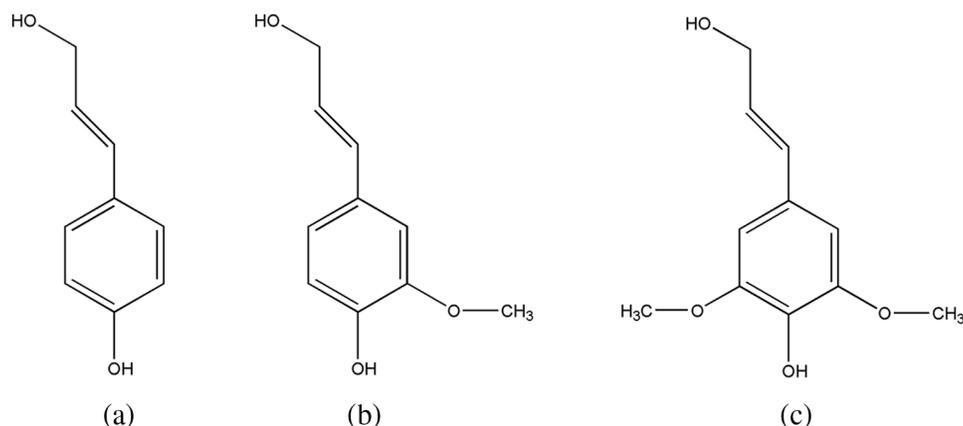
Figure 1: Structural units of lignin, (a) p-hydroxyphenyl propane, (b) guaiacyl, (c) syringyl

2 Materials and Methods

2.1 Materials

Bayberry (*Myrica rubra (Lour.) S. et Zucc*) tannin extract powder was purchased from Jinshan Tannin Company (Tai'an, China). Furfuryl alcohol (FA, with a purity of 98%), formaldehyde (with a purity of 37%), p-toluenesulfonic acid (pTSA, with a purity of 97.5%), and ether (with a purity of 99.5%) were obtained from Sinopharm, China. Tween 80 and guar gum (viscosity of 5000–5500 mPa·s) were purchased from Shandong Kepler Biotechnology Co., Ltd., Shandong, China. Lignin extracted from corn (*Zea mays* L.) stalk residue after the hydrolysis of hemicelluloses was supplied by Long Live Biological Technology Company (Shandong, China), with the following composition: 92.33% Klason lignin, with p-hydroxyphenyl propane as the main monomer structure, 5.38% acid-soluble lignin, and 2.29% cellulose.

2.2 Formulation and Processing of Various Thermosetting Foams

The preparation of TFF foam was performed by addition of 30, 20, and 10 g of tannin, FA, and formaldehyde, respectively, into a beaker while applying homogeneous stirring. Then, 2 g of guar gum (as a release agent and stabilizer) and 4 g of Tween 80 (as a foam stabilizer) were added, manual stirring (HM-955) was continued in the beaker with a low speed (50 r/min) stirrer. Additionally, 15 mL of pTSA (30% aqueous solution) and 2 g of ether as a foaming agent were added into the mixture under stirring for 3 s. After that, the mixture was injected into a mold with 90 mm diameter and 110 mm height and transferred to an oven for foaming and curing at 60°C for 6 h to finally obtain the TFF foam. The preparation of tannin–lignin–furfuryl alcohol-formaldehyde (TLFF) foam was similar to that of TFF foam, with the difference that lignin was used on the expense of 10% of tannin.

The tannin–furfuryl alcohol-glyoxal (TFG) foam was prepared by charging 20 g FA and 10 g glyoxal into a beaker under stirring for 5 min. Then, 30 g tannin and 15 mL of pTSA (30% aqueous solution) were post-added into this mixture while stirring is applied for 2 min to obtain the TFG resin matrix. Then, 2 g of guar gum (as a release agent and stabilizer) and 4 g of Tween 80 (as a foam stabilizer) were added and a low speed stirring (50 r/min) at by manual stirrer ((HM-955) was employed in the beaker. Subsequently, 2 g of ether was added as a foaming agent and mixed well via stirring for 3 s to obtain a foam system with uniform sized pores. The foam liquid was injected into a mold (90 mm diameter and 110 mm height) then transferred into an oven for foaming and curing at 60°C for 6 h. Likewise, the preparation of tannin–lignin–furfuryl alcohol-glyoxal (TLFG) foam was similar to that of TFG foam, with the difference that lignin was used to replace 10% of tannin. A schematic illustration for the preparation of the TLFG foam is shown in Scheme 1. Five repetitions of various foam samples were prepared for testing.
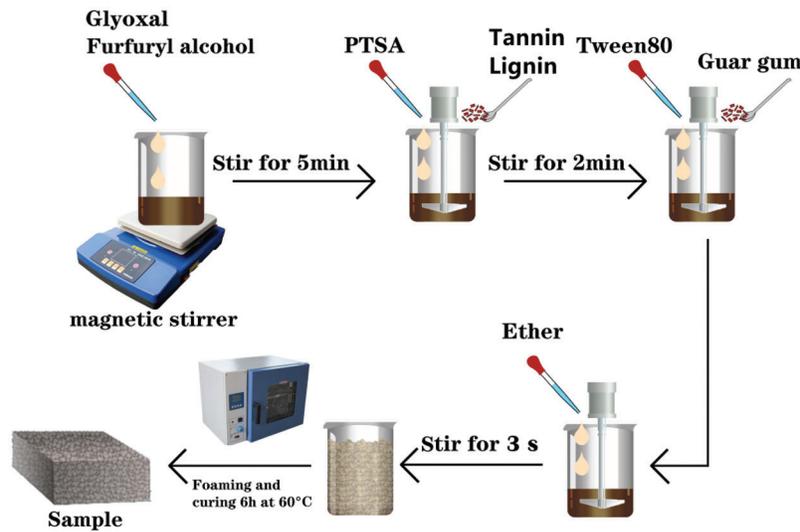
Scheme 1: Schematic illustration for the preparation of a foam based on TLFG resin matrix

2.3 Characterizations

All foams were conditioned at 20°C and a relative humidity of 50% for 24 h before testing. The foam layer was characterized after cutting, and the average value of five repetitions was considered for each test.

The determination of the apparent density for each foam sample was conducted according to the provisions of the national standard GB/T 6342-2009. The size of the prepared sample was measured, and the following formula was applied for calculating the apparent density:

$$\rho = \frac{m}{V} \times 10^6 \tag{1}$$

where, m is the mass of the sample (g); V is the volume of the sample (mm^3); ρ is the apparent density (kg/m^3), and the accuracy limit of the results is around 0.1 kg/m^3.

The thermal conductivity of each foam sample was measured using YBF-2 apparatus (Dahua Ltd., Hangzhou, China) according to Eq. (2)

$$\lambda = -mc\frac{2h_p + R_p}{2h_p + 2R_p} * \frac{1}{\pi R^2} * \frac{h}{T_1 - T_2} * \frac{dT}{d\tau}|T = T_2 \tag{2}$$

where λ represents the thermal conductivity, m and c signify the mass and specific heat capacity of the bottom copper plate of the instrument, respectively. R (50 mm) and h (10 mm) represent the radius and thickness of the specimen after cutting with a sharp knife, respectively, while Rp (50 mm) and hp (10 mm) refer to the radius and thickness of the bottom copper plate, respectively. T1 − T2 indicates the difference between the temperatures of the bottom and top copper plates, and $\frac{dT}{d\tau}|T = T_2$ represents the cooling rate of the copper plates after exposure to air.

The test of the degree of pulverization for each type of foam was undertaken according to the national standard GB/T 12812-2006 and the literature [23]. The prepared foam samples were cut into cubes of (5 ± 0.5) cm × (5 ± 0.5) cm × (5 ± 0.5) cm, on the foam surface for two pulverization tests, one is along the direction of the bubble growth (the longitudinal direction test) and second is perpendicular to the growth direction (transverse direction test). Thus, the foam was displaced in 400 mesh sandpaper with a length of 250 mm, and a 200 g iron prop was put above the foam. The foam was pulled from the beginning of the sandpaper to the end and traveled 30 times repeatedly. The quantity of remaining foam

was recorded and the degree of pulverization is calculated according to Eq. (3)

$$M_f = \frac{m_1 - m_0}{m_1} \times 100\% \tag{3}$$

where m_1 is the original mass of the sample (g), m_0 is the mass of the sample after the test (g), and M_f is the degree of pulverization (%).

The microstructure of foam samples with a size of 1 mm × 1 mm × 1 mm was studied using Hitachi S-4160 FE-scanning electron microscope (SEM) while varian-1000 infrared spectrometer (Varian, Palo Alto, USA) was used to analyze characteristic functional groups of the foams over a wavenumber range from 700 to 4000 cm^{-1} after mixing 1 g KBr with 0.01 g of cured resin matrix powder to prepare the test samples with the shape of sheets.

The ESI-MS was used to measure the chemical structure of the foams. The detection was undertaken using a Waters Xevo Triple Quadrupole-MS Spectrometer (Waters, Milford, MA, USA) equipped with an electrospray ionization source (ESI). The N-(2)-L-alanyl-L-glutamine, TFG resin or TLFG resin, and their mixture samples were dissolved in chloroform sequentially at a concentration of approximately 10 µL/mL and injected into the ESI source plus ion trap mass spectrometer (Bruker Daltonics Inc., Billerica, MA, USA) via a syringe at a flow rate of 5 µg/s. The spectra were recorded in a positive mode, with ion energy of 0.3 eV.

Thermogravimetric analyzer (TGA), model TG 209 F3, NETZSCH, Germany, was implemented to investigate the thermal decomposition behavior of the various cured resin matrixes of the foams in the range from 30°C to 800°C at a heating rate of 20 °C/min under nitrogen atmosphere.

Dynamic thermo mechanical analysis (DMA), NETZSCH, DMA242E, Germany, with DMA 242E Artemis software, was used to assess the glass transition temperature of the relevant cured resin matrixes of the foams. It was operated at a heating rate of 20 °C/min for a temperature range from 80°C to 250°C.

Furthermore, 0.05 g resin matrix of each foam sample was loaded into differential scanning calorimeter (204F1DSC, Germany) to study the curing behavior of the samples under nitrogen as a protective gas in a temperature range from 30°C to 180°C while a heating rate of 15 °C/min was operated.

The compression strength test of each foam sample was accomplished according to the national standard GB/T 8813-2008. Each sample was cut into the size of (30 ± 0.5) mm × (30 ± 0.5) mm × (15 ± 0.5) mm to ensure that the surface of the test sample was smooth while the working area of the mechanical testing machine should be greater than the stressed area of the sample to be tested. The universal mechanical testing machine was adjusted to obtain a compression rate of 2.0 mm/min. Two tests were implemented with one keeping the bubble growth direction of the foam parallel to the pressure direction (longitudinal direction test) while the second was performed while keeping bubble growth direction perpendicular to the pressure direction (transverse direction test).

3 Results and Discussion

Fig. 2 shows the morphology and microstructure of various prepared foams. It is clear that the foam surface in case of TFF is smoother than that of the TFG, which can be correlated with the higher activity of formaldehyde with respect to glyoxal. Moreover, TLFG and TLFF foams appeared smoother than TFF and TFG foams, indicating that the foam prepared with lignin replacing some tannin has more uniform distribution of pores. For each foam system, the addition of ether in presence of Tween 80 while applying intensive mechanical stirring can generate bubbles on the surface and in the bulk of the resin matrix. The foamed liquid was heated in the oven. During the curing process of the mixture, bubbles were generated in the cured mixture, forming a stable network structure. The formation of foam can be divided into three basic processes: bubble nucleation, bubble growth, and foam curing [25,26]. The stage of bubble

nucleation is the key step for formation of high quality foam. This step determines to which extent a uniform distribution of bubbles nuclei is formed at the beginning. The gas could even spread to several nuclear bubbles through strong mechanical stirring, and a fine uniform cell structure can be obtained. To further investigate the internal structure of these foams, SEM was used to observe the microstructure of the foams (Fig. 2). Compared to TLFF foam, several closed and open cells with cracks (marked with blue circle) in the TFF foam, beside parts of collapsed cells (marked with green rectangle) are observed. However, only a few cracks on closed-cells were found in TLFF foam (marked with blue circle). Meanwhile, some cracks and big collapse (marked with green rectangle) were observed on closed cells of TFG foam, whereas only few cracks and no collapses were observed on the closed and open-cells of TLFG foam. Furthermore, the TLFF foams appear to present a higher proportion of closed cells than the others, however, still present a certain proportion of open cells. These results indicate that the foam prepared with some lignin proportion does not affect the distribution of the bubbles, but increases the number of closed cells without cracks or collapses.
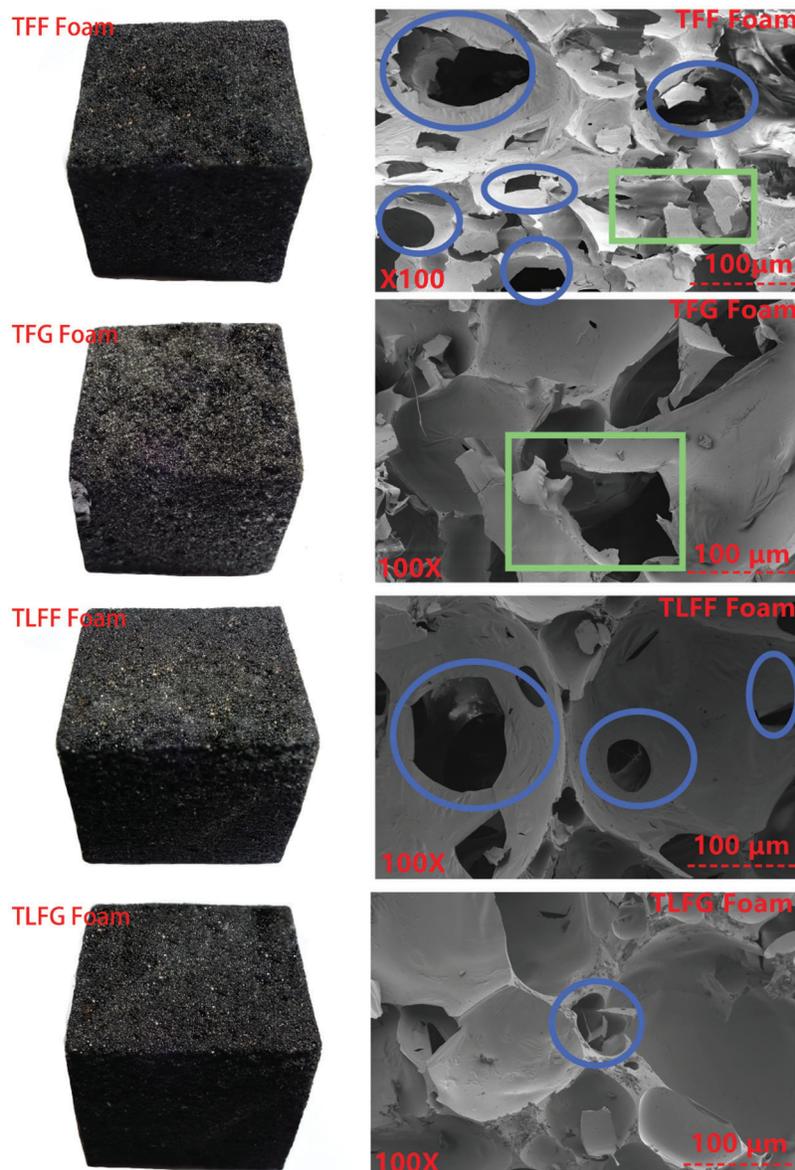
Figure 2: Scanning electron microscopy images of various prepared foams

The apparent density can indirectly reflect the distribution of bubbles and cell size within the foams. The apparent density is inversely proportional to the cell size, which determines the range of its uses [24]. Fig. 3 shows the apparent density of TFF, TFG, TLFF, and TLFG foams prepared in this study. The apparent density of the TFG foam (81.24 ± 4.29 kg/m³) is close to that of the TFF foam (79.78 ± 4.35 kg/m³), indicating that the weight and cell size of foam prepared with glyoxal is close to that of the foam prepared with formaldehyde. Meanwhile, using parts of lignin to replace tannin in the TFG or TFF resin system could make the cells of the foam smaller and have more closing cells without cracks (see SEM of Fig. 2), and increase the weight of the foam. The reason is that the addition of lignin dose leads to complexity in the polymerization reaction during the foaming process of the resin matrix. Thus, the treatment with ether and Tween 80 decreases the size of bubble cells and increases the apparent density of the foams.
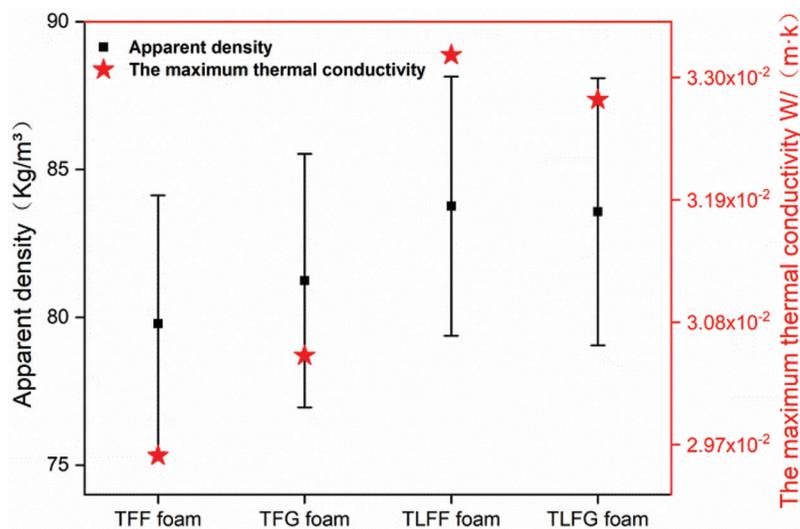

Figure 3: Apparent density and maximum thermal conductivity of various foams

The thermal conductivity value is obtained from the heat transferred through a unit horizontal cross-sectional area per unit time when the heat is stably transferred, which is the significant parameter for foam application. Fig. 3 shows the thermal conductivity of various prepared foams. The thermal conductivity values of TFG and TFF foams are 0.0305 and 0.0296 W/(m·K), respectively, indicating that glyoxal can replace formaldehyde as a crosslinking agent to obtain a similar effect. Moreover, lignin, which is used to replace some tannin, increased the thermal conductivity of the TFF and TFG foams. SEM results showed that the presence of lignin as part of the resin matrix for preparation of TLFG foam decreased the amount of cracks and collapse on closed and open cells of TLFG foam, thus increased the thermal conductivity compared to the TFG foam. However, the TLFG foam is still a good thermal insulating material compared to polystyrene foam (with a thermal conductivity in the range of 0.03–0.04 W/(m·K)) and other types of tannin foam (with a thermal conductivity of 0.02–0.035 W/(m·K)) [27–29].

Fig. 4 shows the transverse and longitudinal stress–strain curves of the prepared foams. It is clear from the figure that the initial part, which is the linear elastic stage of these foams, is reaching the ultimate stress at around 8% strain. Then the yield stage started even under a low stress. Therefore, the stress–strain relation of the foam is relatively flat at this stage. When the strain reaches the range of 52%–55%, a third stage of foam densification was started, where all cell walls have collapsed. It can be observed from Figs. 4a and 4b that the longitudinal stress is larger than the transverse one for each foam. This is attributed to the longitudinal shape

acquired by the rise of internal gas during the foaming stage. The number of longitudinal bubbles per unit area is greater than that of the horizontal bubbles; thus, the foam has a greater compressive strength in the longitudinal direction. The compressive strength of TFF foam is 0.152 MPa in the transverse direction whereas 0.325 MPa in the longitudinal direction, which is higher than that of the TFG foam (0.142 MPa in the transverse direction and 0.286 MPa in the longitudinal direction). Moreover, after adding lignin, the compressive strength of TLFG foam in both directions (transverse of 0.171 MPa and longitudinal of 0.375 MPa) was higher than that of TFG. Similarly, the test result of the TLFF foam was higher than that of the TFF foam. The stressed structure of the foam is produced by internal filling of the triangular intersection between the cell walls of foam. The addition of lignin effectively improves the strength of the cell structure; thus, considered as an effective way for improving the mechanical properties of these foams. Although the compressive strength of TLFG foam is lower than that of the TLFF foam, it has better compressive strength than the tannin-furanic foam prepared in our previous study, in which it was synthesized without a foaming agent (transverse of 0.150 MPa) [24].
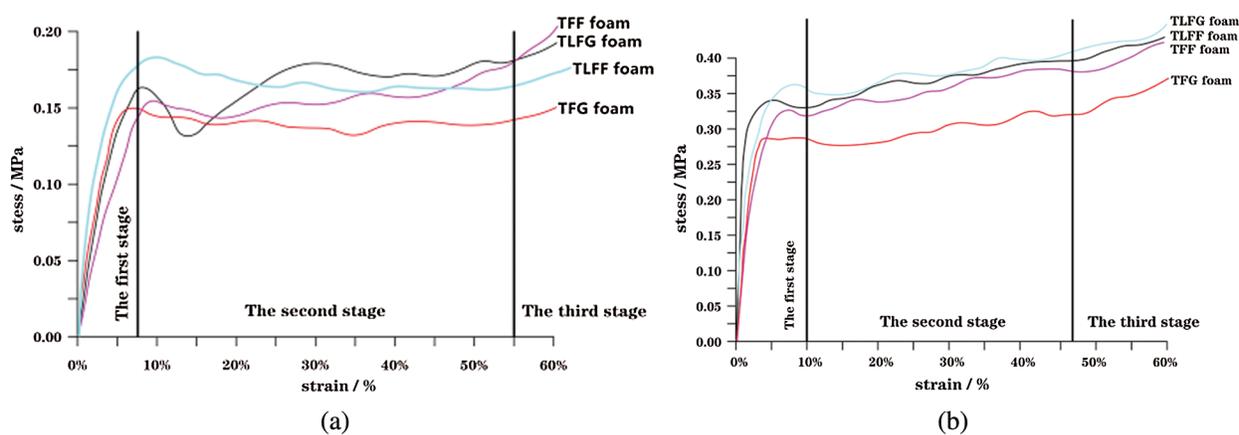
Figure 4: Stress–strain characteristics for the various foams, (a) transverse direction, (b) longitudinal direction

The pulverization degree plays a significant role in foam application, reflecting the foam's softness and hardness and the easiness to drop slag. If the slag dropping rate of the foam is high, it will cause harm to the foams' processing, cutting, and application [25]. Table 1 shows that, for all foams, the longitudinal pulverization degrees are higher than the transverse pulverization ones, indicating that grinding along the direction of the bubble growth and more area of pore walls are in contact with sandpaper, thereby increasing the wear resistance and decreasing the pulverization degree. Additionally, the pulverization degree in the longitudinal (22.39%) and the transverse (18.62%) directions for TFG foam are higher than that of TFF foam. Moreover, the longitudinal and transverse pulverization degrees of TLFG are lower than that of TFG. These results are proportional to the apparent density; the apparent density of the TFG foam is higher than that of the TFF foam. Similarly, the apparent density of TLFG foam is higher than that of the TFG foam, indicating that the foams with the same size and higher apparent density acquire smaller pore size, which causes more area of walls to contact with the sandpaper to reduce the pulverization degree. Thus, parts of lignin that replaced tannin could decrease the pulverization degree.

Table 1: Pulverization degree for various foams in transverse and longitudinal directions

Type	Transverse pulverization degree (%)	Longitudinal pulverization degree (%)
TFF foam	20.25 ± 4.62	17.96 ± 2.64
TLFG foam	17.86 ± 3.96	14.35 ± 1.58
TLFF foam	18.34 ± 4.07	14.59 ± 2.13
TFG foam	22.39 ± 4.18	18.62 ± 2.43

Differential scanning calorimetry (DSC) is a useful technique for studying the impact of any component on the curing process of resin systems. Based on the corresponding thermograms of TFF, TFG, TLFF, and TLFG resins acquired at a heating rate of 10 K/min (Fig. 5), all synthesized resins exhibited exothermic peaks after freeze-drying treatment. The curing temperature of the TFF resin (153°C) was close to that of the TFG resin (150°C). However, the curing temperature of the TLFF resin (136°C) was significantly higher than that of the TLFG resin (105°C). Moreover, cross-linking between tannin, lignin, furfural, and glyoxal proceeds under acidic conditions at a temperature lower than the cross-linking between tannin, furfural, and glyoxal under acidic conditions.
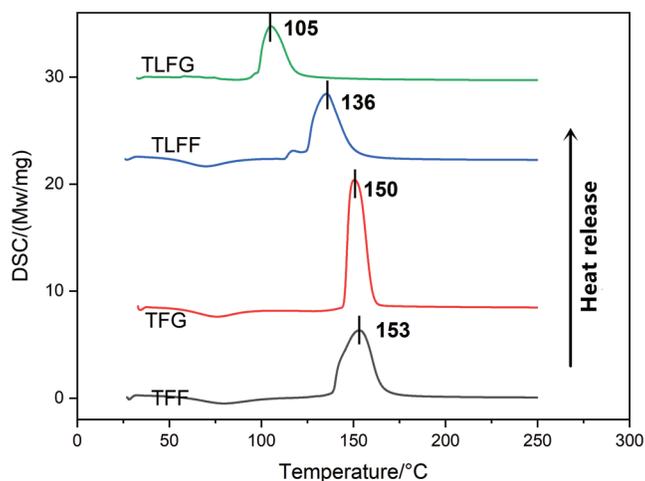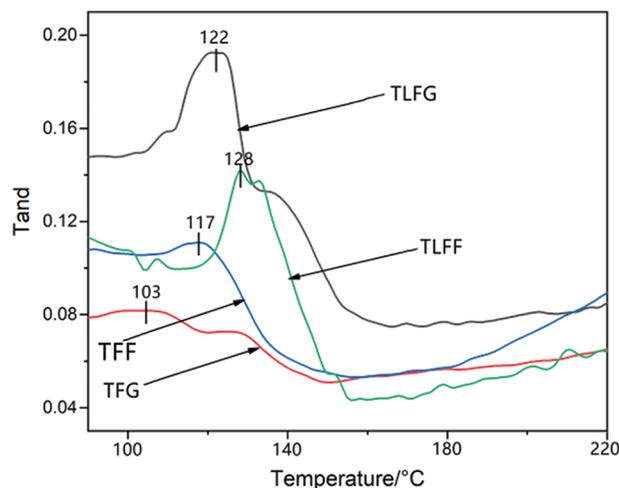

Figure 5: DSC curves of various resin matrixes of the prepared foams

Fig. 6 shows the loss tangent (tan d) curves of cured TFG, TFF, TLFG, and TLFF resins using DMA analysis. The glass transition temperature (Tg) is defined as the maximum value of tan d, and tan d = E''/E', where E'' is the loss modulus, and E' is the storage modulus [30]. The results show that Tg of TLFG resin (122°C) is lower than that of TLFF resin (128°C). Similarly, Tg of TFG resin (103°C) is lower than that of TFF resin (117°C). Thus, indicating that the activity of formaldehyde is higher than that of glyoxal, and the addition of formaldehyde can produce more effective cross-linking with tannin and lignin. Moreover, Tg of TLFG resin is higher than that of TFF and TFG resin, indicating that parts of lignin replacing tannin can increase the heat resistance. To better illustrate the heat resistance of these foams, they were investigated using TGA in the range 30°C to 800°C, and the results are displayed in Fig. 7. The thermogravimetric traces reveal that these foams have high thermal resistance. Under a nitrogen atmosphere and a temperature of 250°C, their weight losses are less than 20%. When the temperature rises to 500°C, the remaining masses are greater than 40%. As clear from the figure, the heat

resistance of TLFG and TLFF foams is higher than that of TFG as well as TFG foams, indicating that the addition of lignin improves the heat resistance of tannin resin-based foam.

Figure 6: DMA traces of various cured resin matrixes of the foams
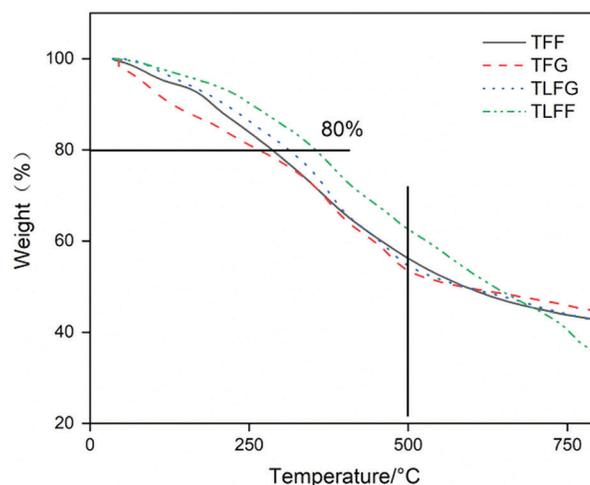

Figure 7: TGA curves of the different foams

The results of DMA and TGA signify that TLFG foam is a good candidate for preparing a novel bio-based foam considering balanced properties of reasonable thermal resistance and upgraded mechanical strength.

FTIR spectroscopy is used to analyze the structure of these resins, and their spectra are exhibited in Fig. 8. For all resins, the stretching vibration absorption peaks generated at a wavenumber of 1606 to 1635 cm^{-1} are attributed to the symmetrical stretching vibration of the C=C belonging to the benzene ring of along with the bending vibration of the O–H bond of tannin and lignin monomer. For the TLFF and TLFG resins, the peak at 1384 cm^{-1} belongs to the bending vibration peak of C–H of the methoxy group, indicating that lignin has an electrophilic reaction with furan ring under acidic conditions. The absorption peak at 1352 cm^{-1} in TFF, TFG, TLFF, and TLFG resins belongs to the bending vibration of C–H in the methylene bridge bond, indicating that the furan ring of FA reacts with the phenolic hydroxyl

groups of tannin to form methylene bridge bond while water is splitted. The absorption peaks at 1190 and 1122 cm^{-1} in TLFF and TLFG resins are derived from C–O–C symmetric and antisymmetric stretching vibrations, indicating that the hydroxymethyl groups on FA units are produced by aldol condensation reaction with formaldehyde or glyoxal. It also indicates that lignin well reacts with tannin to form ether bonds.
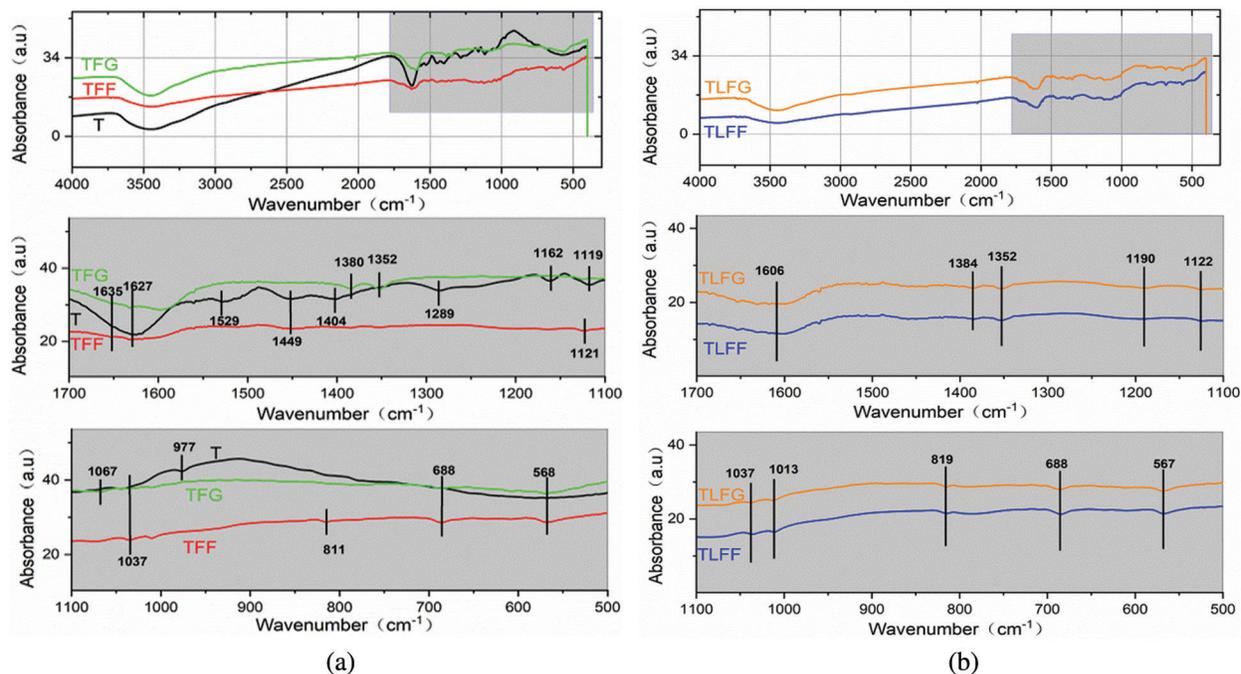

Figure 8: FTIR spectra of various cured resin matrixes of the prepared foams; (a) T, TFF and TFG; (b) TLFF and TLFG

The results of the ESI-MS analysis of the oligomers that were formed during the preparation of the TFG and TLFG foams, are presented in Fig. 9. The main chemical structures of TFG and TLFG are collected in Table 2. All the peak values were based on the molecular weight of the species + 23 Da due to the Na$^+$ ion of the NaCl matrix enhancer used or + 1 Da due to the H$^+$ protonation, while the obtained results suggested the formation of several possible products or intermediates. It can be seen that the peaks at 397 Da and 413 Da, which appear in Figs. 9a and 9b can be attributed to ether and its complexes with three or four oxygen atoms, which is due to the addition of ether as a foaming agent. In addition, from the Fig. 9b, it can be seen that the peak at 291 Da belongs to oligomers formed by condensation of furfuryl alcohol, glyoxal and lignin. Moreover, the peak at 578 Da can be attributed to products of the co-reaction among tannin, furfuryl alcohol, glyoxal and lignin. The phenol hydroxyl group at Carbon 4 of lignin can react with Carbon 4 of furfuran ring, and the alcohol hydroxyl group at Carbon 1 of lignin was etherified with Carbon 8 of tannin. These results indicate that compared with TFG foam, lignin participates efficiently in the reaction system for preparation of TLFG foam to form a dense three-dimensional network structure. Based on the above analysis, the main ongoing reactions in TLFG resin system is assumed in Scheme 2.
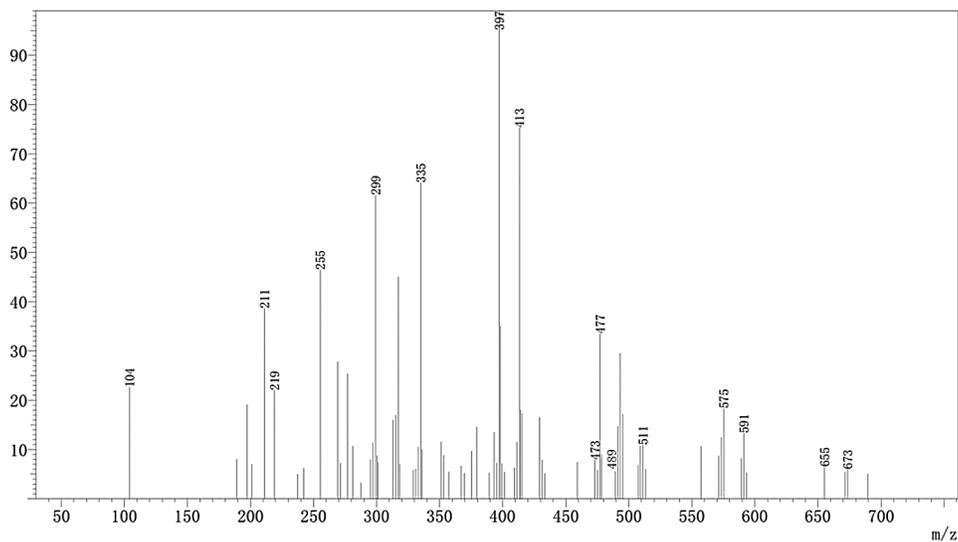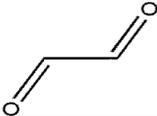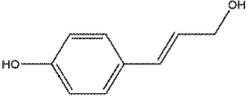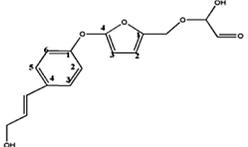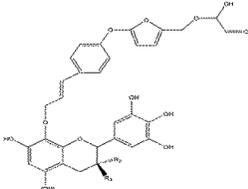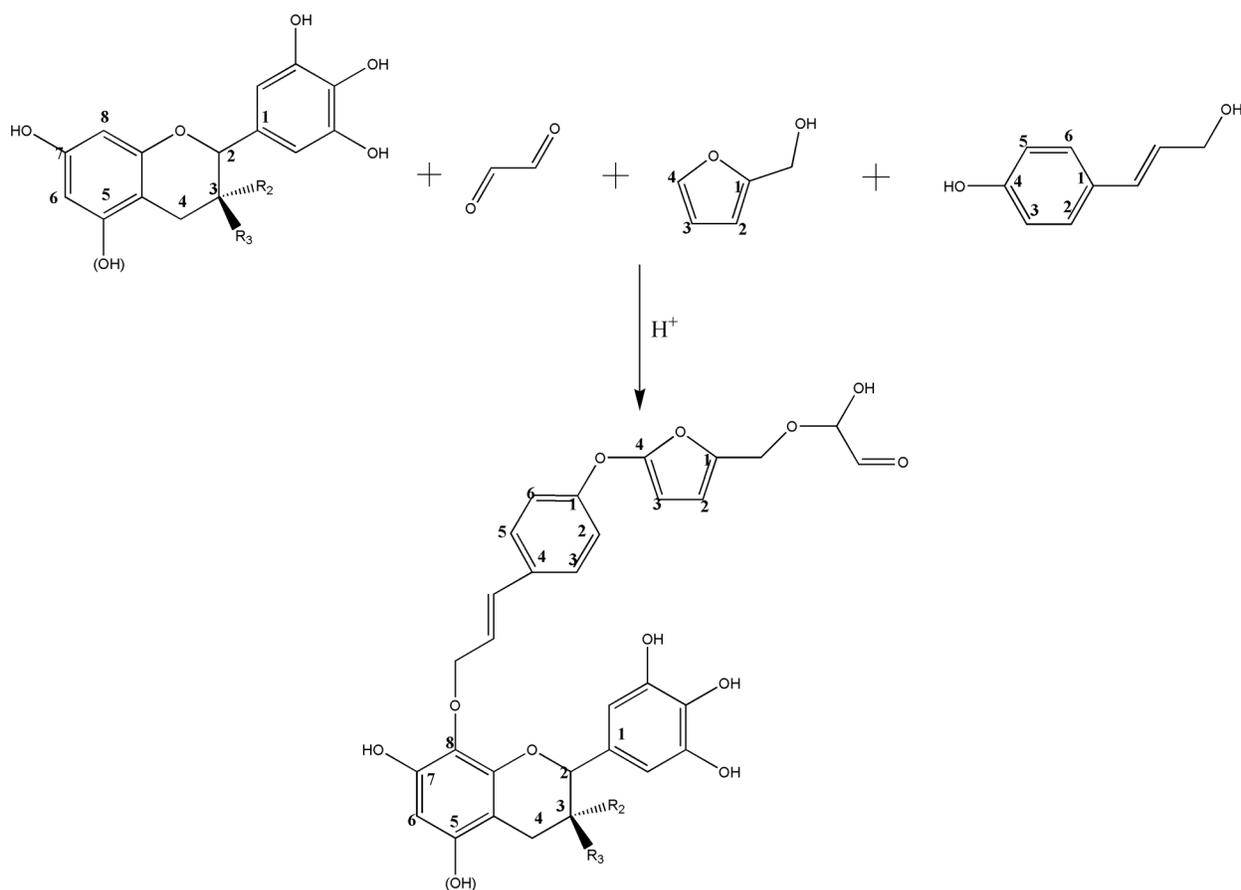
(a)
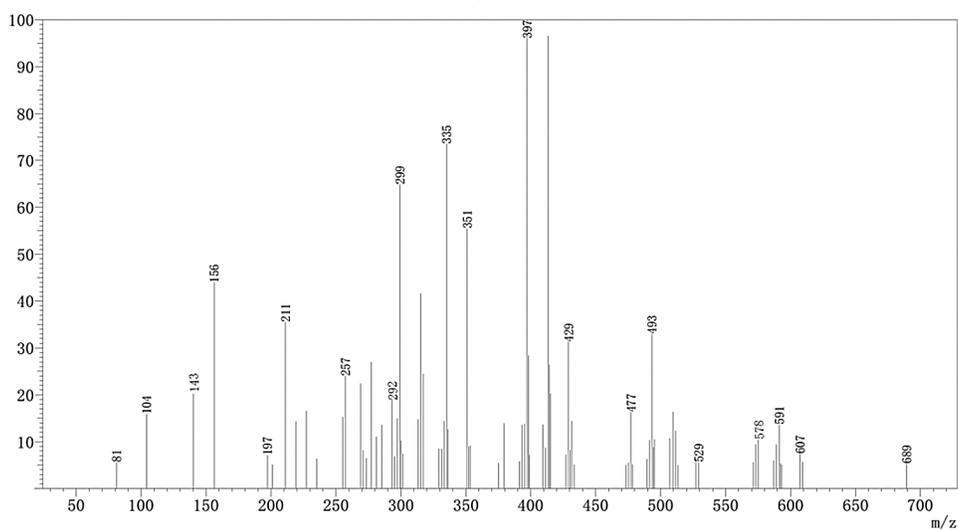
(b)

Figure 9: ESI-MS spectrum of the various prepared foams; (a) TFG; (b) TLFG

Table 2: Oligomers identified by ESI-MS for the reaction of tannin, furfuryl alcohol, glyoxal and lignin

Experimental		Calculated		Chemical species
$[M+H]^+$	$[M+Na]^+$	$[M+H]^+$	$[M+Na]^+$	
	81		81	

(Continued)

Table 2 (continued)

Experimental		Calculated		Chemical species
[M+H]⁺	[M+Na]⁺	[M+H]⁺	[M+Na]⁺	
156		156		
292		292		
578		578		

Scheme 2: Condensation reactions proceeding among tannin, furfuryl alcohol, glyoxal and lignin

4 Conclusions

A novel TLFG foam can be prepared by incorporation of lignin to take part, at the expense of part of tannin, in the condensation reactions with tannin, FA, and glyoxal, which reduces the cost as well as the curing temperature and enhances the heat resistance of the foam. The ongoing condensation reaction between these species generates bonds such as [–C–O–C–] or [–CH$_2$–O–] as elucidated from the FTIR and ESI-MS investigation. Moreover, the produced TLFG foam presents a lower pulverization degree with respect to TFG foam, which signifies a more complicated network structure and prevents harmful effects to the foams' during processing, cutting, and application. This also leads to improved compressive strength compared with that of TFG foam. Thus, the modified TFG resin with lignin became more liable for industrial applications, particularly foam.

Author Contributions: Formal analysis and writing—original draft, Jun Zhang; supervision, Yunxia zhou, Shang Feng and Xuehui Li; review & editing, Hisham Essawy and Xiaojian Zhou.

Conflicts of Interest: The authors declare that they have no conflicts of interest to report regarding the present study.

References

1. Carbone, M., Beaugendre, M., Koral, C., Manikas, A. C., Koutroumanis, N. et al. (2021). Thermoplastic polyurethane-graphene nanoplatelets microcellular foams for electromagnetic interference shielding. *Graphene Technology, 5(3–4),* 33–39. DOI 10.1007/s41127-020-00034-0.

2. Pu, Y. H., Xie, Z. F., Ye, H., Shi, W. (2021). Amidation modified waste polystyrene foam as an efficient recyclable adsorbent for organic dyes removal. *Water Science & Technology, 83(1),* 2192–2206. DOI 10.2166/wst.2021.129.

3. Chen, G., Liu, J., Zhang, W., Han, Y. M., Zhang, D. R. et al. (2021). Lignin-based phenolic foam reinforced by poplar fiber and isocyanate-terminated polyurethane prepolymer. *Polymers, 13(7),* 1068. DOI 10.3390/polym13071068.

4. Lombardi, L., Tammaro, D. (2021). Effect of polymer swell in extrusion foaming of low-density polyethylene. *Physics of Fluids, 33(3),* 033104. DOI 10.1063/5.0035033.

5. Pasch, H., Pizzi, A., Rode, K. (2001). MALDI-TOF mass spectrometry of polyflavonoid tannins. *Polymer, 42(18),* 7531–7539. DOI 10.1016/S0032-3861(01)00216-6.

6. Zhou, X. J., Li, B., Xu, Y., Essawy, H., Wu, Z. G. et al. (2019). Tannin-furanic resin foam reinforced with cellulose nanofibers (CNF). *Industrial Crops and Products, 34(11),* 107–112. DOI 10.1016/j.indcrop.2019.03.052.

7. Tondi, G., Pizzi, A., Pasch, H., Celzard, A. (2008). Structure degradation, conservation and rearrangement in the carbonisation of polyflavonoid tannin/furanic rigid foams—A MALDI-TOF investigation. *Polymer Degradation & Stability, 93(5),* 968–975. DOI 10.1016/j.polymdegradstab.2008.01.024.

8. Lacoste, C., Pizzi, A., Laborie, M. P., Celzard, A. (2014). Pinus pinaster tannin/furanic foams: Part II. Physical properties. *Industrial Crops & Products, 61(1–3),* 531–536. DOI 10.1016/j.indcrop.2014.04.034.

9. Pizzi, A., Tondi, G., Pasch, H., Celzard, A. (2008). Matrix-assisted laser desorption/ionization time-of-flight structure determination of complex thermoset networks: Polyflavonoid tannin-furanic rigid foams. *Journal of Applied Polymer Science, 110(3),* 1451–1456. DOI 10.1002/app.28545.

10. Celzard, A., Zhao, W., Pizzi, A., Fierro, V. (2010). Mechanical properties of tannin-based rigid foams undergoing compression. *Materials Science & Engineering A, 527(16–17),* 4438–4446. DOI 10.1016/j.msea.2010.03.091.

11. Abdullah, U. H. B., Pizzi, A. (2013). Tannin-furfuryl alcohol wood panel adhesives without formaldehyde. *European Journal of Wood & Wood Products, 71(1),* 131–132. DOI 10.1007/s00107-012-0629-4.

12. Zhang, J., Xi, X. D., Liang, J. K., Pizzi, A., Du, G. B. et al. (2019). Tannin-based adhesive cross-linked by furfuryl alcohol-glyoxal and epoxy resins. *International Journal of Adhesion and Adhesives, 94(1),* 47–52. DOI 10.1016/j.ijadhadh.2019.04.012.

13. Liang, J. K., Li, T. H., Cao, M., Lei, H., Du, G. B. (2017). The ESI-MS analysis of furfuryl alcohol and formaldehyde in the acid and alkali mediums. *Journal of Southwest Forestry University (Natural Sciences), 37(6),* 201–209. DOI 10.11929/j.issn.2095-1914.2017.06.031.

14. Li, J. X., Liao, J. J., Essawy, H., Zhang, J., Li, T. H. et al. (2021). Preparation and characterization of novel cellular/nonporous foam structures derived from tannin furanic resin. *Industrial Crops and Products, 162(1),* 113264. DOI 10.1016/j.indcrop.2021.113264.

15. Lacoste, C., Basso, M. C., Pizzi, A., Laborie, M. P., Garcia, D. et al. (2013). Bioresourced pine tannin/furanic foams with glyoxal and glutaraldehyde. *Industrial Crops and Products, 45,* 401–405. DOI 10.1016/j.indcrop.2012.12.032.

16. Calco-Flores, F. G., Dobado, J. A. (2010). Lignin as renewable raw material. *ChemSusChem, 3(11),* 1227–1235. DOI 10.1002/cssc.201000157.

17. Dongre, P., Driscoll, M., Amidon, T., Bujanovic, B. (2015). Lignin-furfural based adhesives. *Energies, 8(8),* 7897–7941. DOI 10.3390/en8087897.

18. Stewart, D. (2008). Lignin as a base material for materials applications: Chemistry, application and economics. *Industrial Crops and Products, 27(2),* 202–207. DOI 10.1016/j.indcrop.2007.07.008.

19. Xue, B. L., Wen, J. L., Sun, R. C. (2014). Lignin-based rigid polyurethane foam reinforced with pulp fiber: Synthesis and characterization. *ACS Sustainable Chemistry & Engineering, 2(6),* 1474–1480. DOI 10.1021/sc5001226.

20. Turnnen, M., Alvila, L., Pakkanen, T. T., Rainio, J. (2003). Modification of phenol-formaldehyde resol resins by lignin, starch, and urea. *Journal of Applied Polymer Science, 88(2),* 582–588. DOI 10.1002/(ISSN)1097-4628.

21. Toni, V., Henrik, R., Tero, L., Tuomo, H., Ulla, L. (2020). Characterization of lignin enforced tannin/furanic foams. *Heliyon, 6(1),* e03228. DOI 10.1016/j.heliyon.2020.e03228.

22. Panigrahi, D., Kumar, S., Dhar, A. (2019). Modulating chain conformations of polyvinyl alcohol through low cost and nontoxic glyoxal crosslinker: Application in high performance organic transistors. *Organic Electronics, 65,* 193–200. DOI 10.1016/j.orgel.2018.11.017.

23. Xu, Y. (2019). *Preparation and modification of Bayberry tannin rigid foam (Master Thesis)*, pp. 18–19. Southwest Forestry University.

24. Li, J. X., Liao, J. J., Zhang, J., Zhou, X. J., Essawy, H. et al. (2020). Effect of post-added water amount on pre-concentrated bark foaming materials by mechanical stirring. *Journal of Renewable Materials, 8(12),* 1607–1616. DOI 10.32604/jrm.2020.013976.

25. Zhao, W., Pizzi, A., Fierro, V., Du, G. B., Celzard, A. (2010). Effect of composition and processing parameters on the characteristics of tannin-based rigid foams. Part I: Cell structure. *Materials Chemistry & Physics, 122(1),* 175–182. DOI 10.1016/j.matchemphys.2010.02.062.

26. Chen, G., Liu, J., Zhang, W., Han, Y. M., Zhang, D. R. et al. (2021). Lignin-based phenolic foam reinforced by poplar fiber and isocyanate-terminated polyurethane prepolymer. *Polymers, 13(7),* 1068. DOI 10.3390/polym13071068.

27. Basso, M. C., Li, X., Fierro, V., Pizzi, A., Giovando, S. et al. (2011). Green, formaldehyde-free, foams for thermal insulation. *Advanced Materials Letters, 2(6),* 378–382. DOI 10.5185/amlett.2011.4254.

28. Sayadi, A. A., Tapia, J. V., Neitzert, T. R., Clifton, G. C. (2016). Effectsof expanded polystyrene (EPS) particles on fire resistance, thermal conductivity and compressive strength of foamed concrete. *Construction and Building Materials, 112(6),* 716–724. DOI 10.1016/j.conbuildmat.2016.02.218.

29. Zhang, H., Fang, W. Z., Li, Y. M., Tao, W. Q. (2017). Experimental study of the thermal conductivity of polyurethane foams. *Applied Thermal Engineering, 115(2),* 528–538. DOI 10.1016/j.applthermaleng. 2016.12.057.

30. Merino, D., Simonutti, R., Perotto, G., Athanassiou, A. (2021). Direct transformation of industrial vegetable waste into bioplastic composites intended for agricultural mulch films. *Green Chemistry, 23(16),* 5956–5971. DOI 10.1039/D1GC01316E.